



Contents lists available at ScienceDirect

Arabian Journal of Chemistry

journal homepage: www.ksu.edu.sa

Identification of *Miscanthus floridulus* as a promising anti-Alzheimer's disease and antidiabetic agent through bioactivity evaluations and chemical composition analyses

Dingping Zhao^{a,b,1}, Qijun Dai^{c,1}, Yuanyuan Zhang^{a,b,1}, Hongjian Shen^{a,b}, Yan Mao^{a,b}, Xianxian Zhou^{a,b}, Xiqing Chen^{a,b}, Hanqing pang^{a,b}, Hui Wang^{d,e,f,*}, Liang Liu^{a,b,**}

^a Institute of Translational Medicine, School of Medicine, Yangzhou University, Yangzhou 225009, China

^b Jiangsu Key Laboratory of Integrated Traditional Chinese and Western Medicine for Prevention and Treatment of Senile Diseases, Yangzhou University, Yangzhou 225009, China

^c Department of Neurology, Haian Hospital of Traditional Chinese Medicine, Haian 226600, China

^d College of Life Sciences, Anhui Normal University, Wuhu 241000, China

^e Anhui Provincial Key Laboratory of the Conservation and Exploitation of Biological Resources, Anhui Normal University, Wuhu 241000, China

^f Key Laboratory of Biomedicine in Gene Diseases and Health of Anhui Higher Education Institutes, Anhui Normal University, Wuhu 241000, China

ARTICLE INFO

Keywords:

Poaceae

Biological activity

Chemical composition

Miscanthus floridulus

LC-IT-TOF-MS

ABSTRACT

The Poaceae family, the fifth largest family of angiosperms, has always been an important source of cereal crops, medicinal crops, and industrial crops. However, comprehensive studies on the biological activity and chemical composition of many species are lacking. In the present study, we tested the total flavonoid and total phenol contents and antioxidant, α -glycosidase, α -amylase, acetylcholinesterase (AChE), and butyrylcholinesterase (BChE)-inhibitory activities of five Poaceae plants (*Echinochloa crus-galli*, *Miscanthus floridulus*, *Sporobolus fertilis*, *Bromus japonicus*, and *Eleusine indica*). As a result, the 95 % ethanol (EtOH) extract of *M. floridulus* (EMF) was found to possess strongest abovementioned activities among the extracts of the five different species. The IC₅₀ value of the DPPH radical scavenging activity was $23.18 \pm 0.36 \mu\text{g/mL}$, and those of the anti-AChE, anti-BChE and anti- α -glycosidase activities were 49.92 ± 1.44 , 100.37 ± 2.48 , and $50.01 \pm 2.15 \mu\text{g/mL}$, respectively. Forty-four compounds were identified from the EMF through liquid chromatography-hybrid ion trap-time of flight mass spectrometry (LC-IT-TOF-MS) analysis, and the majority of these compounds were flavonoids and organic acids. In general, the obtained results highlight the medicinal value of the five members of the Poaceae family. More importantly, *M. floridulus* has potential for the development of multitarget anti-Alzheimer's disease (AD) and antidiabetic agents in the pharmaceutical industry.

1. Introduction

The inhibition of enzymes in some metabolic pathways is the key attribute for treatment of some health problems (Grochowski et al., 2017, Cetin et al., 2021). Alzheimer's disease (AD) and diabetes are two common chronic diseases that attract great attention in public health areas, imposing a heavy burden on society and the economy. One of the most critical markers in the definitive diagnosis of AD is cholinergic loss due to decrease in the secretion of acetylcholine (ACh), a crucial

neurotransmitter in the brain (Lahiri et al., 2003, Balci et al., 2023). Acetylcholinesterase (AChE) and butyrylcholinesterase (BChE) are hydrolytic enzymes, and their primary role is the hydrolysis of choline esters, including ACh (Ferreira-Vieira et al., 2016, Balci et al., 2023). Coinhibiting AChE and BChE are essential in prolonging choline activity at synapses (Balci et al., 2023), providing directions for the development of new anti-AD drugs. The inhibition of α -amylase and α -glucosidase can delay glucose absorption, which result in low postprandial plasma blood glucose and prevents postprandial hyperglycemia (Yilmaz et al., 2023).

* Corresponding author at: College of Life Sciences, Anhui Normal University, Wuhu 241000, China.

** Corresponding author at: Institute of Translational Medicine, School of Medicine, Yangzhou University, Yangzhou 225009, China.

E-mail addresses: wh741230@ahnu.edu.cn (H. Wang), liuliang@yzu.edu.cn (L. Liu).

¹ These authors contributed equally to this work.

<https://doi.org/10.1016/j.arabjc.2024.106037>

Received 7 July 2024; Accepted 26 October 2024

Available online 29 October 2024

1878-5352/© 2024 The Authors. Published by Elsevier B.V. on behalf of King Saud University. This is an open access article under the CC BY license (<http://creativecommons.org/licenses/by/4.0/>).

Synthetic enzyme inhibitors for AD and diabetes treatment in the clinic have exhibited serious side effects, including gastrointestinal disturbances and toxicity. Therefore, new safe alternative compounds from natural resources are urgently needed (Stefanucci et al., 2020).

The diverse chemical constituents of plants are considered great sources of enzyme inhibitors (Yilmaz et al., 2023). The Poaceae family is the fifth largest family of angiosperms; it has a long history of domestication and is the most economically valuable family in the plant kingdom. The Poaceae family comprises approximately 10,000 species and is grown abundantly worldwide. This large family has always been an important source for the grain industry, pharmaceutical industry and animal husbandry and has greatly contributed to the survival and development of humans (Gallaher et al., 2022, Huang et al., 2022). However, knowledge of the chemical profiles and bioactivities of many species in the Poaceae family is still lacking, which has severely hindered further development and utilization of plant resources from this family.

Echinochloa crus-galli (L.) P. Beauv., *Miscanthus floridulus* (Lab.) Warb. ex Schum et Laut., *Sporobolus fertilis* (Steud.) W. D. Glayt., *Bromus japonicus* Thunb. ex Murr., and *Eleusine indica* (L.) Gaertn. are members of the Poaceae family. They are widely distributed worldwide and used as pasture or medicinal plants (Fujian Institute of Medicine 1970, Zhang et al., 2008, El Molla et al., 2016, Ong et al., 2017, Mala et al., 2022). However, the chemical profiles and bioactivities of these species remain poorly defined. Related studies have shown that plants of the Poaceae family contain flavonoids and phenols, which are important types of secondary metabolites and possess multiple biological activities, including α -glycosidase, α -amylase, AChE, and BChE-inhibitory and antioxidant activities. The principles of plant chemical taxonomy reveal that closely related species contain similar or even identical chemical components. Therefore, we hypothesize that the five Poaceae plants may contain flavonoids and phenols and possess the abovementioned bioactivities.

To confirm this speculation, in the present study, 95 % ethanol (EtOH) extracts of *E. crus-galli* (EEC), *M. floridulus* (EMF), *S. fertilis* (ESF), *B. japonicus* (EBJ) and *E. indica* (EEI) were obtained via heat under reflux. The chemical constituent contents (total flavonoid and total phenol contents) and bioactivities (antioxidant, anti-AChE, anti-BChE, anti- α -glucosidase, and anti- α -amylase activities) of the different extracts were subsequently determined. Finally, liquid chromatography-hybrid ion trap-time of flight mass spectrometry (LC-IT-TOF-MS) was carried out to analyze the chemical profile of the extract with the strongest tested activities. Combined together, this study aims to

elucidate the phytochemical profile and bioactivity of these five plants and provide a theoretical basis for better utilizing plants from the Poaceae family.

2. Materials and methods

2.1. Plant materials

Whole grasses of five species were collected from Anhui Province, China, in July 2022. The grasses were identified as *E. crus-galli*, *M. floridulus*, *S. fertilis*, *B. japonicus*, or *E. indica* (Fig. 1) by Dr. Hui Wang from Anhui Normal University. Voucher samples (EC20220708, MF20220708, SF20220708, BJ20220708, and EI20220708) were deposited in the herbarium of the School of Medicine of Yangzhou University.

2.2. Sample preparation

The whole grasses of *E. crus-galli*, *M. floridulus*, *S. fertilis*, *B. japonicus*, and *E. indica* were pulverized into powders and extracted with 95 % EtOH four times at 85 °C for 2 h each time by the hot reflux method to obtain the corresponding crude extracts. For LC-IT-TOF-MS analysis, approximately 10.0 mg of each extract was sonicated for 30 min at 100 Hz, followed by filtration through a 0.22 μ m Millipore filter before use. The 18 chemical compounds were weighed and dissolved in 70 % methanol. Then, an assimilated standard sample was obtained by mixing the single standard solutions.

2.3. Chemicals and reagents

Quercetin, luteolin, apigenin, diosmetin, baicalein, and gallic acid were purchased from Must Biotechnology Co., Ltd. (Chengdu, China). Quinic acid, malic acid, *trans*-5-O-caffeoylquinic acid, 4-hydroxycinnamic acid, isoorientin, rutin, isovitexin, isoquercetin, cynaroside, eriodictyol, naringenin, kaempferide, and emodin were purchased from Pufeí De Biotechnology Co., Ltd. (Chengdu, China). α -Glucosidase, acarbose, and α -amylase were purchased from Sigma-Aldrich Chemical Co. (St. Louis, MO, USA). Vitamin C, 2,2-diphenyl-1-picrylhydrazyl (DPPH), and 2,2'-azino-bis-(3-ethylbenzothiazoline-6-sulfonic acid) (ABTS) were purchased from Bomei Biotechnology Co., Ltd. (Hefei, China). Electric eel AChE, horse serum BChE, acetylthiocholine iodide, S-butrylthiocholine iodide, and 5',5-dithio-bis(2-nitrobenzoic acid) (DTNB) were purchased from Yuanye Biotechnology Co., Ltd.

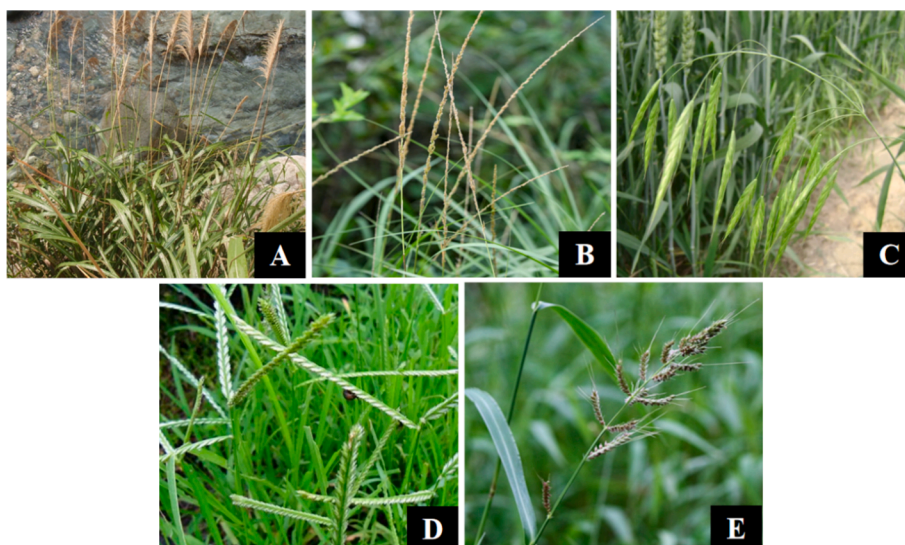


Fig. 1. Pictures of five Poaceae plants. (A) *Miscanthus floridulus*. (B) *Sporobolus fertilis*. (C) *Bromus japonicus*. (D) *Eleusine indica*. (E) *Echinochloa crus-galli*.

(Shanghai, China). Sodium dodecyl sulfate (SDS), phosphate-buffered saline (PBS), and galanthamine were purchased from Solarbio Co., Ltd. (Beijing, China). 4-Nitrophenyl- α -D-glucopyranoside (PNPG) was purchased from Macklin Biotechnology Co., Ltd. (Shanghai, China).

2.4. Determination of the total phenol and total flavonoid contents

The total phenol contents of EEC, EMF, ESF, EBJ and EEI were determined by the Folin–Ciocalteu method (Qneibi et al., 2021). Folin–Ciocalteu solution (2.5 mL, 0.1 mM) was added to 2.5 mL of the sample solution and incubated for 6 min. Then, 150 μ L of Na₂CO₃ solution (200 mg/mL) was added to the mixed solution, followed by a reaction at room temperature for 2 h. The absorbance was measured at 765 nm by an EnSpire Multilabel Reader (PerkinElmer). The total phenol content was calculated with reference to a standard curve for gallic acid (Abs = 0.0104 [GA] + 0.037, R² = 0.9993). The results are expressed as gallic acid equivalents (mg GAE/g dry weight of extract).

The total flavonoid contents of EEC, EMF, ESF, EBJ and EEI were determined using a UV–visible spectrophotometer. The sample solution (1 mL) was mixed with 4 mL of 30 % EtOH and 0.3 mL of NaNO₂ (50 mg/mL). After 6 min of incubation, 300 μ L of 10 % Al(NO₃)₃·9H₂O was added, and the mixture was incubated for another 6 min. Then, 4.0 mL of NaOH solution (100 mg/mL) was added to the mixture, and 60 % EtOH was added to reach a volume of 10.0 mL. The absorbance was measured at 510 nm after 30 min. The total flavonoid content of the sample was calculated according to a standard curve generated from freshly prepared rutin solutions of different concentrations, ranging from 10–50 μ g/mL (Abs = 0.755 [R] + 0.0435, R² = 0.9996). The results are expressed as rutin equivalents (mg RUE/g dry weight of extract).

2.5. Evaluation of in vitro antioxidant activity

DPPH/ABTS assays were performed to determine the in vitro antioxidant capacities of EEC, EMF, ESF, EBJ and EEI via methods described in previous studies (Xu et al., 2020, Zhang et al., 2021). The samples (100 μ L) were mixed with an equal volume of DPPH/ABTS radical solution. After reacting at 37 °C in the dark for 30 min (DPPH) or 5 min (ABTS), the absorbance of each sample was measured at 517 nm (DPPH) or 734 nm (ABTS). The sample and EtOH (both 100 μ L) were mixed in the control group. DPPH/ABTS and EtOH (both 100 μ L) were mixed in the blank group. The sample concentrations in the DPPH assay were 400, 200, 100, 50, and 25 μ g/mL. The concentrations used in the ABTS assay were 2000, 1000, 500, 250, and 125 μ g/mL. Vitamin C served as the positive control. The free radical scavenging rates were calculated using the following equation:

$$\text{Free radical scavenging rate} = [1 - (\text{OD}_1 - \text{OD}_2)/\text{OD}_3] \times 100 \%$$

where, OD₁, OD₂, and OD₃ are the absorbances of the sample and DPPH/ABTS, sample and EtOH, and DPPH/ABTS and EtOH, respectively.

2.6. AChE/BChE inhibition assay

The AChE/BChE-inhibitory activity was determined according to

Table 1

Total phenol/flavonoid contents of 95% EtOH crude extracts of *Echinochloa crus-galli* (EEC), *Miscanthus floridulus* (EMF), *Sporobolus fertilis* (ESF), *Bromus japonicus* (EBJ) and *Eleusine indica* (EEI).

Samples	Total phenol content (mg GAE/g)	Total flavonoid content (mg RUE/g)
EEC	27.92 ± 0.60	73.25 ± 3.42
EMF	74.34 ± 2.84	147.79 ± 3.18
ESF	48.50 ± 0.56	71.63 ± 1.23
EBJ	61.71 ± 0.91	102.02 ± 6.03
EEI	33.26 ± 0.90	87.23 ± 3.77

Table 2

In vitro antioxidant activities of EEC, EMF, ESF, EBJ and EEI.

Samples	ABTS	DPPH
EEC	1591.86 ± 54.57	168.81 ± 2.60
EMF	276.48 ± 8.82	23.18 ± 0.36
ESF	806.46 ± 29.70	48.97 ± 1.43
EBJ	261.07 ± 1.51	64.27 ± 2.70
EEI	866.96 ± 25.23	80.37 ± 0.48
Vitamin C	14.19 ± 0.14	2.06 ± 0.096

IC₅₀ values, μ g/mL for EEC, EMF, ESF, EBJ and EEI; μ M for the positive control vitamin C.

methods described previously (Zou et al., 2021, Liu et al., 2022). PBS solution (100 μ L, pH 8.0), acetylthiocholine iodide or butyrylthiocholine iodide (20 μ L, 1.2 mM), AChE or BChE (20 μ L, 0.05 U/mL), and sample solution (20 μ L) were added in turn to a 96-well plate and then incubated at 37 °C for 30 min. SDS (20 μ L, 4 %) was added to the well to terminate the reaction, followed by the addition of DTNB (20 μ L, 0.6 mM). Afterward, the absorbance of each sample was immediately measured at 517 nm. Galanthamine served as the positive control. The inhibition rate of the sample was estimated using the following formula:

$$\text{Inhibition rate} = [1 - (\text{OD}_1 - \text{OD}_2)/(\text{OD}_3 - \text{OD}_4)] \times 100 \%$$

where, OD₁, OD₂, OD₃, and OD₄ are the absorbance of the sample, the absorbance of the sample without AChE/BChE, the absorbance of AChE/BChE, and the absorbance in the absence of sample and AChE/BChE, respectively.

2.7. α -Glucosidase inhibition assay

The α -glucosidase assay was performed following protocols described in previous publications (Xu et al., 2020, Liu et al., 2022). Sample solution (24 μ L), PBS solution (96 μ L, 0.1 mol/L), and α -glucosidase solution (10 μ L) were added to the wells. The mixture was reacted at 37 °C for 15 min, and then PNPG solution (30 μ L) was added to the mixture. After reacting at 37 °C for another 20 min, the reaction was terminated by adding 80 μ L of Na₂CO₃ solution (0.2 mol/L). The absorbance of each sample was measured at 405 nm. Acarbose was used as the positive control. The equation used in the AChE/BChE-inhibitory assays was used to calculate the α -glucosidase inhibition rate.

2.8. α -Amylase inhibition assay

The α -amylase assay was performed following protocols described in previous publications (Meng et al., 2016, Liu et al., 2022). Sample solution (50 μ L) and α -amylase solution (50 μ L) were mixed in a glass test tube. After reacting in a water bath at 37 °C for 10 min, starch solution (50 μ L) was added to the mixture, which was then allowed to react at 37 °C for another 10 min. Afterward, 1 mL of 3,5-dinitrosalicylic acid solution was added to the tube, and the final mixture was reacted in boiling water for 10 min, followed by cooling to room temperature. The absorbance of each sample was measured at 540 nm. The equation for the AChE/BChE-inhibitory assays was used to calculate the percentage of α -amylase inhibition.

2.9. LC–IT–TOF–MS analysis

The analytical system (Kyoto, Japan) was composed of a Shimadzu LC–MS/MS system, which included two LC–20AD_{XR} pumps, a DGU–20A_{3R} degasser, an SIL–20AC_{XR} autosampler, and a hybrid ion trap-time of flight–mass spectrometer (IT–TOF–MS). A Waters Acquity UPLC HSS T3 column (2.1 × 100 mm, 1.8 μ m, Milford, MA, USA) was connected to an electrospray ionization (ESI) interface and used for chromatographic separations. The mobile phase consisted of solvents A (0.1 % formic acid in water) and B (acetonitrile) and was used for

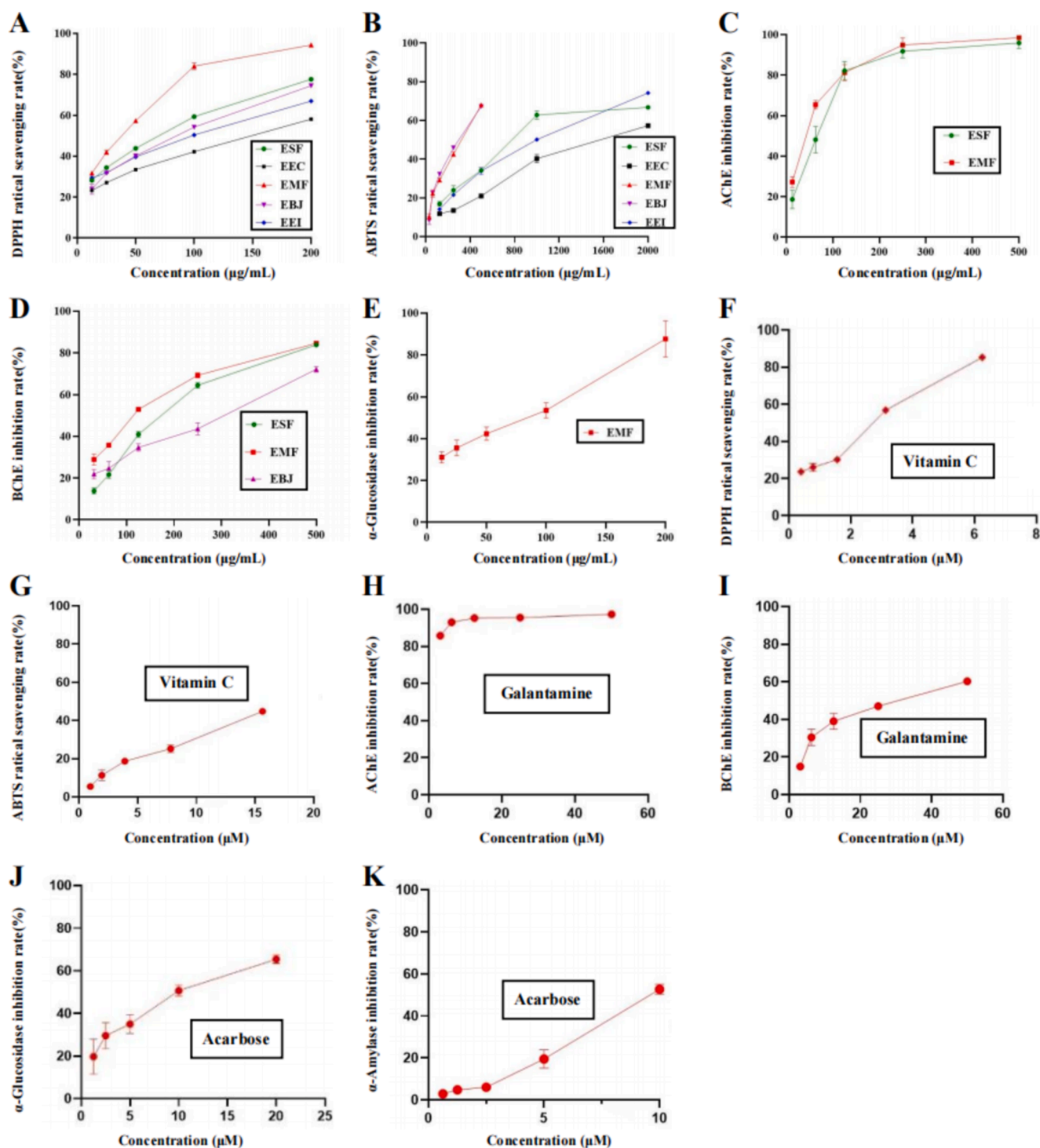


Fig. 2. Multiple activities of five different extracts. (A and B) DPPH and ABTS radical scavenging activities of 95 % ethanol extracts of *E. crus-galli* (EEC), *M. floridulus* (EMF), *S. fertilis* (ESF), *B. japonicus* (EBJ) and *E. indica* (EEL). (C and D) AChE and BChE inhibitory activities of EMF, ESF and EBJ. (E) α -Glucosidase inhibitory activity of EMF. (F and G) DPPH and ABTS radical scavenging activities of vitamin C. (H and I) AChE and BChE inhibitory activities of galatamine. (J and K) α -Glucosidase and α -amylase inhibitory activities of acarbose. The data are presented as the means \pm S.E.M.s.

gradient elution. The elution method was as follows: 0–5 min, 95–85 % A; 5–13 min, 85–72 % A; 13–23 min, 72–5 % A; 23–25 min, 5 % A; and 25–30 min, 5–95 % A. The temperature of the column was controlled at 40 °C, the flow rate was set to 0.2 ml/min, and the injection volume was set to 3 μ l.

The following mass spectrometric parameters were used: nitrogen was used as the nebulizing gas and drying gas, with a nebulizing gas flow rate of 1.45 L/min and a drying gas pressure of 100 MPa. Furthermore, a

curved desolvation line (CDL) voltage was set at a constant level, with a CDL temperature of 200 °C, a block heater temperature of 200 °C, an interface voltage of 1.40 kV, a detector voltage of 1.45 kV and an IT vacuum of 1.9×10^{-2} Pa. The collision energy during collision-induced dissociation (CID) was maintained at 50 %, and 100 ms was set as the ion accumulation time. The samples were analyzed in both positive and negative ion modes over a m/z range of 100 to 1000 Da via LCMS solution software (Version 3, Shimadzu).

Table 3

Enzyme inhibitory activities of EEC, EMF, ESF, EBJ and EEI.

Samples	AChE	BChE	α -Glucosidase	α -Amylase
EEC	Na	Na	Na	Na
EMF	49.92 \pm 1.44	100.37 \pm 2.48	50.01 \pm 2.15	Na
ESF	64.52 \pm 3.27	155.21 \pm 4.34	Na	Na
EBJ	Na	238.42 \pm 3.25	Na	Na
EEI	Na	Na	Na	Na
Galanthamine	0.63 \pm 0.10	10.65 \pm 0.45	Nd	Nd
Acarbose	Nd	Nd	9.25 \pm 0.08	10.53 \pm 0.88

IC₅₀ values, μ g/mL for EEC, EMF, ESF, EBJ and EEI; μ M for the positive controls, galanthamine and acarbose. Na: not available in the range of the tested concentrations. Nd: not determined.

2.10. Statistical analysis

One-way ANOVA followed by Dunnett's test was used to compare differences among groups. All the statistical analyses were carried out using SPSS Version 25.0 for Windows (IBM SPSS Inc., Chicago, IL), and $P < 0.05$ was considered statistically significant. For quantitative analyses, all data are presented as the mean \pm S.E.M. Bioactivity and chemical profile experiments were repeated at least 3 times to confirm their reproducibility.

3. Results and discussion

3.1. Total phenol and total flavonoid contents

The results are shown in Table 1. The total phenol contents of the

EEC, EMF, ESF, EBJ and EEI ranged from 27.92 \pm 0.60 to 74.34 \pm 2.84 GAE/g. The order of total phenol content from high to low was as follows: EMF > EBJ > ESF > EEI > EEC. Moreover, the total flavonoid contents of the EEC, EMF, ESF, EBJ and EEI were in the range of 71.63 \pm 1.23 to 147.79 \pm 3.18 mg RUE/g. The order of total flavonoid content from high to low was as follows: EMF > EBJ > EEI > EEC > ESF. Among all five tested samples, EMF contained the highest phenol and flavonoid contents.

3.2. Antioxidant assays

The antioxidant activity is presented as IC₅₀ values. The smaller the IC₅₀ value is, the stronger the antioxidant activity. According to the data presented in Table 2 and Fig. 2, the IC₅₀ values of the DPPH and ABTS radicals scavenged by EEC, EMF, ESF, EBJ and EEI ranged from 23.18 \pm 0.36 to 168.81 \pm 2.60 μ g/mL and from 261.07 \pm 1.51 to 1591.86 \pm 54.57 μ g/mL, respectively. EMF exhibited the strongest DPPH scavenging ability. In the ABTS assay, the inhibitory activities of EMF and EBJ were almost equal, and EBJ had the strongest ABTS scavenging ability. All the samples scavenged the DPPH radical much more efficiently than the ABTS radical.

3.3. Inhibitory activity of multiple enzymes

As shown in Table 3 and Fig. 2, EMF and ESF showed AChE-inhibitory activities, and their IC₅₀ values were 49.92 \pm 1.44 and 64.52 \pm 3.27 μ g/mL, respectively. In the BChE assay, EMF, ESF and EBJ exhibited inhibitory activities, and their IC₅₀ values were 100.37 \pm 2.48, 155.21 \pm 4.34, and 238.42 \pm 3.25 μ g/mL, respectively. EMF ranked

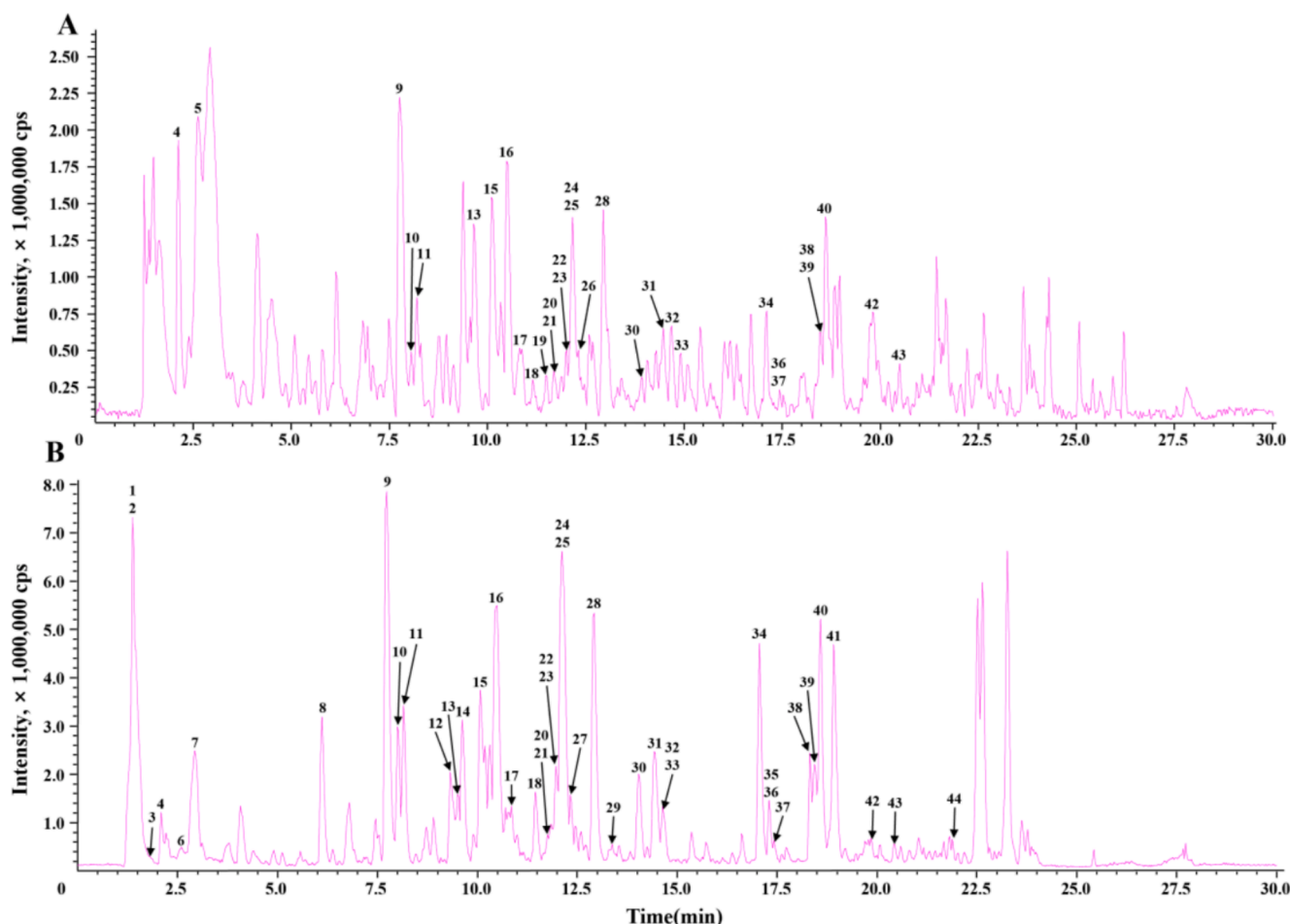


Fig. 3. Typical total ion chromatograms (TICs) of EMF by LC-IT-TOF-MS. (A) positive mode; (B) negative mode.

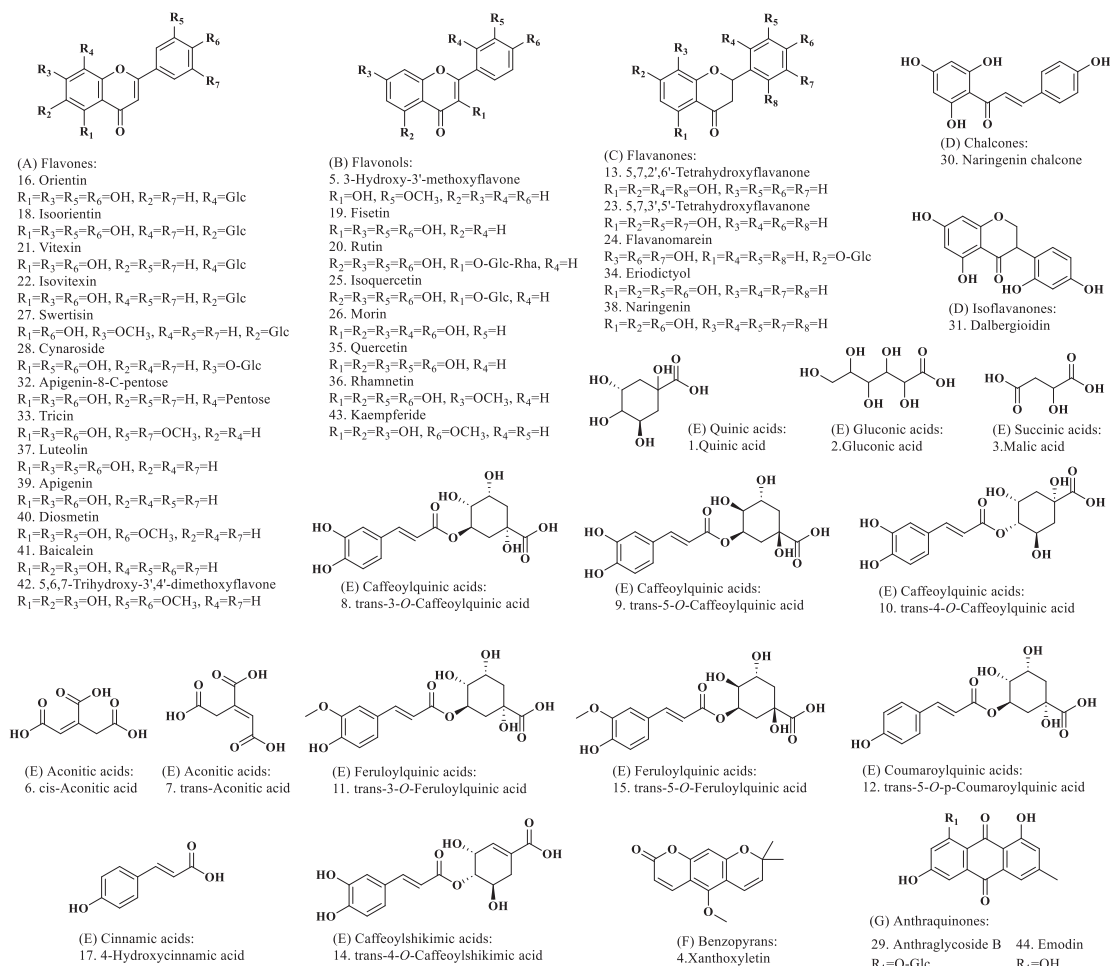


Fig. 4. Chemical structures of the 44 identified compounds.

first in both assays. In the α -glucosidase assay, only EMF was found to exhibit inhibitory activity, and its IC_{50} value was $50.97 \pm 2.15 \mu\text{g/mL}$. In addition, none of the five tested samples exhibited α -amylase-inhibitory activity.

3.4. LC-IT-TOF-MS analysis of EMF

Among the five samples, EMF had the highest total phenol/flavonoid contents and the strongest DPPH radical scavenging, dural anti-AChE and anti-BChE, and selective anti- α -glucosidase activities. The LC-IT-TOF-MS technique was employed to characterize the chemical profile of the EMF. Fig. 3 shows the total ion chromatograms (TICs) of EMF. The identification process for chemical compounds in EMF involved the following steps: (1) extraction of ion features from the raw LC-IT-TOF-MS data for each ion peak in TICs; (2) tentative characterization of the chemical compounds by comparing their ion features, retention times, and mass spectra with those of known chemical compounds in mass bank databases and relevant literature; and (3) to further confirm some identified compounds, their LC-IT-TOF-MS data was compared with those of their corresponding standard chemicals. As a result, a total of 44 compounds were identified, including 13 flavones, 8 flavonols, 5 flavanones, 2 other flavonoids, 13 organic acids, 2 anthraquinones and 1 benzopyran. Among these 44 compounds, 18 were confirmed through chemical standards. Notably, 21 compounds (xanthoxyletin, 3-hydroxy-3'-methoxyflavone, 5,7,2',6'-tetrahydroxyflavanone, orientin, fisetin, vitexin, 5,7,3',5'-tetrahydroxyflavanone, flavanomarein, isoquercetin, morin, swertisin, anthraglycoside B, naringenin chalcone, dalbergioidin, eriodictyol, rhamnetin, diosmetin, baicalein, 5,6,7-trihydroxy-3',4'-

dimethoxyflavone, kaempferide and emodin) were first identified from the genus *Miscanthus*, and 41 compounds (quinic acid, gluconic acid, xanthoxyletin, 3-hydroxy-3'-methoxyflavone, *cis*-aconitic acid, *trans*-aconitic acid, *trans*-3-*O*-caffeoylquinic acid, *trans*-5-*O*-caffeoylquinic acid, *trans*-4-*O*-caffeoylquinic acid, *trans*-3-*O*-feruloylquinic acid, *trans*-5-*O*-*p*-coumaroylquinic acid, 5,7,2',6'-tetrahydroxyflavanone, *trans*-4-*O*-caffeoylshikimic acid, *trans*-5-*O*-feruloylquinic acid, orientin, 4-hydroxycinnamic acid, isoorientin, fisetin, rutin, vitexin, isovitexin, 5,7,3',5'-tetrahydroxyflavanone, flavanomarein, isoquercetin, morin, swertisin, anthraglycoside B, naringenin chalcone, dalbergioidin, apigenin-8-C-pentose, triclin, eriodictyol, rhamnetin, luteolin, naringenin, apigenin, diosmetin, baicalein, 5,6,7-trihydroxy-3',4'-dimethoxyflavone, kaempferide and emodin) were first identified from *M. floridulus*. The structures of these identified compounds are depicted in Fig. 4, and their detailed identification information can be found in Table 4. The MS/MS chromatograms of five typical identified compounds can be found in Fig. 5.

3.4.1. Identification of flavones and flavonols in EMF

For mono C-glycoside flavones, a prominent base ion $[M-H-120]^-$ indicated the presence of a hexose molecule at the C-8 position of the aglycone, whereas a base ion $[M-H-90]^-$ was indicative of the 6-C isomer configuration of the same aglycone molecule. For example, P16 (isoorientin, luteolin-6-C-glucoside) and P18 (orientin, luteolin-8-C-glucoside) are two examples of flavone C-glycosides found in EMF. Their precursor ions were both m/z 447 $[M-H]^-$, and the corresponding fragment ions also demonstrated losses of 120 Da (m/z 327) and 90 Da (m/z 357). P16 displayed a stronger abundance for the m/z 357 ion,

Table 4
Characterization of the chemical constituents of EMF.

No.	t _R (min)	Formula	Precursor ions(m/z)	Diff.	Fragment ions(m/z)	Identification*	Structure [#]	Ref.
P1	1.443	C ₇ H ₁₂ O ₆	191.0573 [M-H] ⁻	6.28	173.05,171.03,127.04,111.05,109.03,93.04,85.03,	Quinic acid*	E	(Matsuda et al., 2016)
P2	1.450	C ₆ H ₁₂ O ₇	195.0517 [M-H] ⁻	3.59	195.05,160.84,129.02,	Gluconic acid	E	(Kakazu and Horai 2016)
P3	1.853	C ₄ H ₆ O ₅	133.0141 [M-H] ⁻	-0.75	133.01,115.01,	Malic acid*	E	(Matsuda et al., 2009a)
P4	2.133	C ₁₅ H ₁₄ O ₄	259.0953 [M+H] ⁺	-4.63	201.04,183.03,95.77,	Xanthoxyletin	F	(Phelan 2019)
			257.0812 [M-H] ⁻	-2.72	128.04,			
P5	2.483	C ₁₆ H ₁₂ O ₄	269.0824 [M+H] ⁺	5.95	236.12,218.11,196.09,154.09,	3-Hydroxy-3'-methoxyflavone	B	(Cuthbertson et al., 2016)
P6	2.552	C ₆ H ₆ O ₆	173.0097 [M-H] ⁻	2.89	129.03,111.01,85.03,	cis-Aconitic acid	E	(Tetsuya 2019)
P7	2.842	C ₆ H ₆ O ₆	173.0098 [M-H] ⁻	3.47	129.02,111.02,85.03,	trans-Aconitic acid	E	(Sawada et al., 2008)
P8	6.183	C ₁₆ H ₁₈ O ₉	353.0876 [M-H] ⁻	-0.57	191.06,179.04,135.05,	trans-3-O-Caffeoylquinic acid	E	(Parveen et al., 2014)
P9	7.621	C ₁₆ H ₁₈ O ₉	355.1003 [M+H] ⁺	-5.91	163.04,	trans-5-O-Caffeoylquinic acid*	E	(Parveen et al., 2014)
			353.0867 [M-H] ⁻	-3.12	353.08,191.06,			
P10	8.073	C ₁₆ H ₁₈ O ₉	355.1033 [M+H] ⁺	2.53	163.04,	trans-4-O-Caffeoylquinic acid	E	(Parveen et al., 2014)
			353.0862 [M-H] ⁻	-4.53	191.06,179.04,173.05,135.05,			
P11	8.103	C ₁₇ H ₂₀ O ₉	369.1168 [M+H] ⁺	-3.25	177.05,114.67,66.95,61.76,	trans-3-O-Feruloylquinic acid	E	(Parveen et al., 2014)
			367.1014 [M-H] ⁻	-5.72	194.06,193.05,134.04,			
P12	9.363	C ₁₆ H ₁₈ O ₈	337.0913 [M-H] ⁻	-4.75	191.06,173.04,163.04,	trans-5-O-p-Coumaroylquinic acid	E	(Parveen et al., 2014)
P13	9.592	C ₁₅ H ₁₂ O ₆	289.0696 [M+H] ⁺	-3.81	271.06,253.05,163.04,153.02,135.05,117.03,69.23,	5,7,2',6'-Tetrahydroxyflavanone	C	(Wang 2017)
			287.0553 [M-H] ⁻	-2.79	151.01,			
P14	9.682	C ₁₆ H ₁₆ O ₈	335.0756 [M-H] ⁻	-4.78	335.07,179.04,135.05,	trans-4-O-Caffeoylshikimic acid	E	(Parveen et al., 2011)
P15	10.143	C ₁₇ H ₂₀ O ₉	369.1193 [M+H] ⁺	3.52	225.77,	trans-5-O-Feruloylquinic acid	E	(Parveen et al., 2014)
			367.1024 [M-H] ⁻	-3.00	191.06,173.05,			
P16	10.713	C ₂₁ H ₂₀ O ₁₁	449.1068 [M+H] ⁺	-1.0	431.10,413.09,395.07,383.07,367.07,353.07,329.07,311.05,299.05,	Isoorientin*	A	(Waridel et al., 2001)
			447.0929 [M-H] ⁻	-0.89	429.09,411.49,393.05,369.07,357.06,328.05,327.05,			
P17	10.923	C ₉ H ₈ O ₃	165.0554 [M+H] ⁺	4.85	147.04,95.25,53.83,	4-Hydroxycinnamic acid*	E	(Schulze 2017)
			163.0410 [M-H] ⁻	5.52	120.05,119.06,			
P18	11.452	C ₂₁ H ₂₀ O ₁₁	449.1060 [M+H] ⁺	-4.01	287.05,	Orientin	A	(Waridel et al., 2001)
			447.0925 [M-H] ⁻	-1.79	327.05,309.03,299.06,285.04,284.03,241.05,			
P19	11.482	C ₁₅ H ₁₀ O ₆	287.0551 [M+H] ⁺	-0.35	269.04,241.05,231.06,161.02,153.02,149.03	Fisetin	B	(Kohlhoff, 2016a)
P20	11.733	C ₂₇ H ₃₀ O ₁₆	611.1613 [M+H] ⁺	0.98	303.04,56.71,	Rutin*	B	(Sánchez-Rabeneda et al., 2003)
			609.1462 [M-H] ⁻	0.16	343.05,301.03,271.03,255.03,			
P21	11.793	C ₂₁ H ₂₀ O ₁₀	433.1139 [M+H] ⁺	2.31	416.10,415.10,397.09,367.08,337.07,313.07,283.06,	Vitexin	A	(Waridel et al., 2001)
			431.0984 [M-H] ⁻	0.00	341.06,312.06,311.05,283.05,			
P22	12.022	C ₂₁ H ₂₀ O ₁₀	433.1125 [M+H] ⁺	-0.92	415.10,397.09,379.08,367.08,337.07,313.07,283.06,	Isovitexin*	A	(Waridel et al., 2001)
			431.0982 [M-H] ⁻	-0.46	413.08,353.07,342.07,341.07,323.06,312.06,311.05,298.03,283.06,			
P23	12.093	C ₁₅ H ₁₂ O ₆	289.0679 [M+H] ⁺	-2.8	271.06,253.05,205.05,187.04,179.03,163.04,153.02,145.03,117.03,	5,7,3',5'-Tetrahydroxyflavanone	C	(Nessa et al., 2004)
			287.0552 [M-H] ⁻	-3.14	287.05,152.00,151.01,135.05,			
P24	12.153	C ₂₁ H ₂₂ O ₁₁	451.1225 [M+H] ⁺	-2.22	289.07,285.83,71.06,	Flavanomarein	C	(Matsuda et al., 2009b)
			449.1098 [M-H] ⁻	2.00	449.11,329.06,288.06,287.06,151.01,			
P25	12.273	C ₂₁ H ₂₀ O ₁₂	465.1016 [M+H] ⁺	-2.58	304.04,303.05,	Isoquercetin*	B	(Sánchez-Rabeneda et al., 2003)
			463.0880 [M-H] ⁻	-0.43	302.04,301.03,300.03,			
P26	12.363	C ₁₅ H ₁₀ O ₇	303.0484 [M+H] ⁺	-4.95	257.04,229.05,165.01,153.01,137.03,	Morin	B	(Silva 2019)
P27	12.393	C ₂₂ H ₂₂ O ₁₀	445.1139 [M-H] ⁻	-0.22	325.07,297.04,282.05,231.03,216.01,	Swertisin	A	(Silva 2014)
P28	12.891	C ₂₁ H ₂₀ O ₁₁	449.1090 [M+H] ⁺	2.67	288.04,287.05,86.70,71.73,54.79,	Cynaroside*	A	(Sánchez-Rabeneda et al., 2003)
			447.0934 [M-H] ⁻	0.22	447.09,327.05,286.04,285.04,			
P29	13.402	C ₂₁ H ₂₀ O ₁₀	431.0976 [M-H] ⁻	-1.86	311.06,270.05,269.05,225.04,	Anthraglycoside B	F	(Kang 2018)
P30	13.950	C ₁₅ H ₁₂ O ₅	273.0770 [M+H] ⁺	4.39	153.02,147.04,	Naringenin chalcone	D	(Boettcher 2016)
			271.0605 [M-H] ⁻	-2.58	177.02,151.01,			
P31	14.392	C ₁₅ H ₁₂ O ₆	289.0696 [M+H] ⁺	-3.81	271.06,253.04,205.04,179.04,163.04,153.02,112.60,81.51,68.43,	Dalbergioidin	D	(Wishart et al., 2007)
			287.0551 [M-H] ⁻	-3.48	151.01,			
P32	14.613	C ₂₀ H ₁₈ O ₉	403.1027 [M+H] ⁺	0.74	385.09,367.08,337.07,201.02,85.54,71.98,	Apigenin-8-C-pentose	A	(Parveen et al., 2014)
			401.0897 [M-H] ⁻	4.74	383.07,342.07,341.07,312.06,311.05,			
P33	14.732	C ₁₇ H ₁₄ O ₇	331.0799 [M+H] ⁺	-3.93	315.05,287.06,270.05,130.37,52.03	Tricin	A	(Kohlhoff, 2016b)
			329.0653 [M-H] ⁻	-4.25	314.04,			

(continued on next page)

Table 4 (continued)

No.	t _R (min)	Formula	Precursor ions(<i>m/z</i>)	Diff.	Fragment ions(<i>m/z</i>)	Identification*	Structure [#]	Ref.
P34	17.193	C ₁₅ H ₁₂ O ₆	289.0691 [M+H] ⁺ 287.0559 [M-H] ⁻	-5.54 -0.70	271.06,241.05,187.04,179.04,163.04,153.02,145.03,135.05,117.04, 269.05,151.01,135.05,125.03,	Eriodictyol*	C	(Matsuda, 2016a)
P35	17.313	C ₁₅ H ₁₀ O ₇	301.0345 [M-H] ⁻	-2.99	286.05,179.00,151.01,	Quercetin*	B	(Sánchez-Rabaneada et al., 2003)
P36	17.340	C ₁₆ H ₁₂ O ₇	317.0653 [M+H] ⁺ 315.0529 [M-H] ⁻	-0.95 6.03	317.06,303.04,302.04,274.05,175.64, 301.04,300.03,	Rhamnetin	B	(Matsuda, 2016b)
P37	17.413	C ₁₅ H ₁₀ O ₆	287.0551 [M+H] ⁺ 285.0390 [M-H] ⁻	0.35 -5.26	241.05,161.02,153.02,135.05, 257.05,241.05,223.04,217.05,199.04,175.04,151.01,133.04	Luteolin*	A	(Sánchez-Rabaneada et al., 2003)
P38	18.313	C ₁₅ H ₁₂ O ₅	273.0739 [M+H] ⁺ 271.0620 [M-H] ⁻	-6.96 2.95	153.02,147.04,119.05, 151.00,119.03,	Naringenin*	C	(Zhao et al., 2023)
P39	18.413	C ₁₅ H ₁₀ O ₅	271.0590 [M+H] ⁺	-4.06	229.05,153.02,145.03,119.05,	Apigenin*	A	(Zhao et al., 2023)
P40	18.643	C ₁₆ H ₁₂ O ₆	269.0438 [M-H] ⁻ 301.0703 [M+H] ⁺	-6.32 -1.33	225.06,201.07,183.06,181.06,151.00,149.03, 286.05,258.05,	Diosmetin*	A	(Zhao et al., 2023)
P41	19.213	C ₁₅ H ₁₀ O ₅	299.0562 [M-H] ⁻ 269.0462 [M-H] ⁻	0.33 2.60	284.03,271.03,227.04,203.04,161.03, 269.04,223.04,	Baicalein*	A	(Matsuda, 2016c)
P42	19.803	C ₁₇ H ₁₄ O ₇	331.0791 [M+H] ⁺ 329.0652 [M-H] ⁻	-6.34 -4.56	330.34,316.05,315.05,287.05,270.05,271.06,68.15, 314.04,201.10,171.11,	5,6,7-Trihydroxy-3',4'-dimethoxyflavone	A	(Ji et al., 2004)
P43	20.563	C ₁₆ H ₁₂ O ₆	301.0717 [M+H] ⁺ 299.0579 [M-H] ⁻	3.32 6.02	286.04,259.06,195.02,178.02,138.19,82.02, 284.03,192.01,	Kaempferide*	B	(Matsuda, 2016d)
P44	21.973	C ₁₅ H ₁₀ O ₅	269.0446 [M-H] ⁻	-3.35	271.05,241.05,225.05,211.04,210.03,197.06,181.07,	Emodin*	F	(Kohlhoff, 2016c)

A: Flavones, B: Flavonols, C: Flavonones, D: Other Flavonoids, E: Organic acids, F: Others.

* Compounds that are compared with standards.

whereas P18 exhibited a stronger intensity for the *m/z* 327 ion. Furthermore, the [M-H-H₂O]⁻ ion at *m/z* 429 was absent in P18 but present in P16. Additionally, the [A-H]⁻ ion at *m/z* 285, representing the deprotonation product of the aglycone, was exclusively observed in P18. After their MS/MS spectra and retention time data (see Table 4) were compared with the authentic standards, mass banks and references (Waridel et al., 2001), P16 and P18 were identified as isoorientin and orientin, respectively.

The spectra of both O-glycoside flavones and flavonols revealed the deprotonated glycoside [M-H]⁻ and aglycones [A-H]⁻. In these compounds, the loss of the glycosyl moiety led to the formation of the corresponding aglycone ions.

For example, P28 (cymaroside, luteolin-7-O-glucoside), a type of O-glycoside flavone, exhibited the loss of the glucose unit (*m/z*: 447 → 285) in negative ion mode and a weak signal of internal fragmentation of its sugar moiety (*m/z* 327, indicating [M-H-120]⁻). The product ion spectrum and retention time (see Table 4 and Fig. 5 (A)) revealed the presence of kaempferol or luteolin and confirmed the identity of cymaroside through comparison with its standard.

Similarly, in negative ion mode, two O-glycoside flavonols, rutin (P20, quercetin-3-O-rutinoside), lost the rhamnose-glucose unit with a *m/z* transition of 609 → 301 (see Fig. 5 (B)), and P25 was identified as isoquercetin (quercetin-3-O-glucoside) with a *m/z* of 463 → 301. To confirm the identity of the two compounds, their spectra and retention times (see Table 4) were compared with those of reference standards.

3.4.2. Identification of flavanones in EMF

There is an asymmetric carbon (C-2) in flavanones, which are commonly found in EMF, with multiple hydroxyl groups attached to them. For example, peaks at *m/z* 269, 151 [C₇H₃O₄]⁻ and 135 [C₇H₃O₃]⁻ in the negative ion mode of P34 (eriodictyol, 5,7,3',4'-tetrahydroxyflavanone) suggested the presence of two hydroxyls in both the A and B rings, which corresponded to [M-H-H₂O]⁻, [A₁-H]⁻ and [B₃-H]⁻ ions. After the MS/MS spectrum and retention data (see Table 4 and Fig. 5 (C)) were compared with those of the standard and reference (Matsuda, 2016a), P34 was identified as eriodictyol.

P38 was identified as naringenin (5,7,4'-trihydroxyflavanone) through analysis of its protonated ion at *m/z* 271 [M-H]⁻ and characteristic fragment ions produced by RDA cleavage, which were observed at *m/z* 151 [A₁-H]⁻ and 119 [A₁-H-2O]⁻, indicating two hydroxyls in the A ring. By comparing the observed data (see Table 4) to those of a standard, P38 as identified as naringenin.

3.4.3. Identification of the organic acids in EMF

Quinic acid (QA) is a common compound with antimalarial and antiviral effects. In EMF, the parent ion for P1 (quinic acid) was detected at *m/z* 191 [M-H]⁻, and it produced fragment peaks (see Fig. 5 (D)) at *m/z* 173 [M-H-H₂O]⁻, 127 [M-H-H₂O-H₂O-CO]⁻, 109 [M-H-CH₄O₃-H₂O]⁻ and 93 [M-H-CH₆O₄-O]⁻, which suggested that there were likely at least four hydroxyls and a keto carbonyl group in the molecular structure of the P1, and is consistent with the known structure of quinic acid. P1 was identified as quinic acid after verifying standard and mass bank data (Matsuda et al., 2016).

Caffeoylquinic acid (CQA) compounds are natural phenolic acids formed by the esterification condensation of quinic acid (QA) and caffeic acid (CA) in varying amounts. In negative ion mode, there are two main fragmentation pathways: the first involves cleavage of the carbonyl-oxygen bond, resulting in the [QA-H]⁻ ion at *m/z* 191; the second involves β-elimination of the carboxylic acid, leading to the [QA-H-H₂O]⁻ anion at *m/z* 173 and the [CA-H]⁻ ion at *m/z* 179.

For example, P9 (*trans*-5-O-caffeoylquinic acid) presented a precursor ion at *m/z* 353 [M-H]⁻, which was followed by a product base ion at *m/z* 191 [QA-H]⁻. On the other hand, P8 (*trans*-3-O-caffeoylquinic acid) exhibited a base ion at *m/z* 191 and a prominent [CA-H]⁻ ion peak at *m/z* 179 (see Table 4), indicating that P9 underwent only the first pathway of fragmentation and P8 probably underwent both the first and second

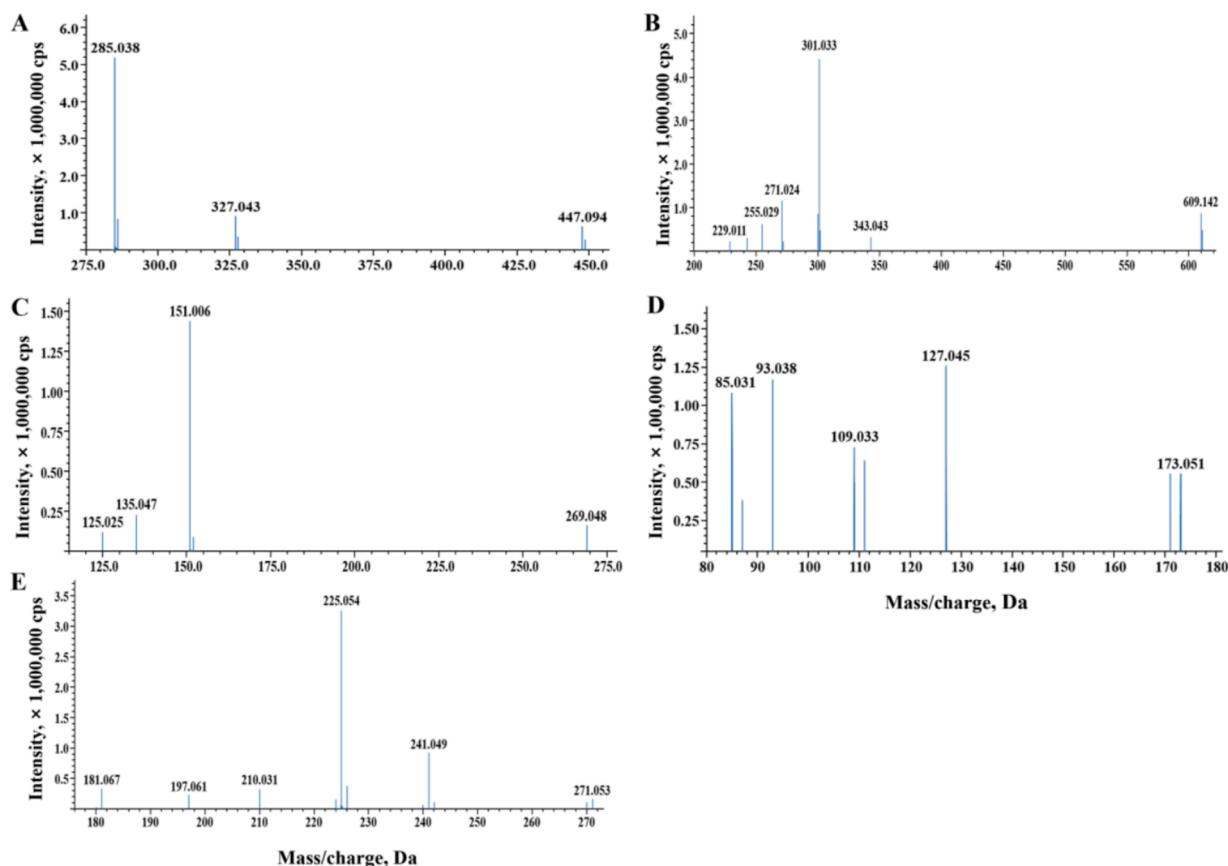


Fig. 5. MS/MS chromatograms of five typical identified compounds. (A) Cynaroside. (B) Rutin. (C) Eriodictyol. (D) Quinic acid. (E) Emodin.

pathways of fragmentation. Furthermore, P10 (*trans*-4-*O*-caffeoylquinic acid) displayed β -elimination of carboxylic acid, resulting in a base ion at $[\text{QA-H-H}_2\text{O}]^-$ m/z 173. These caffeoylquinic acids (P8, P9 and P10) were identified by comparing their spectra and retention times (see Table 4) with those of the corresponding reference and standards (Parveen et al., 2014).

Additionally, other organic acids formed through esterification condensation displayed similar fragmentation pathways. P11 (*trans*-3-*O*-feruloylquinic acid) was characterized by its base ion $[\text{ferulate}]^-$ at m/z 193 resulting from the elimination of the carboxylic acid, whereas P15 (*trans*-5-*O*-feruloylquinic acid) displayed an ion $[\text{QA-H}]^-$ at m/z 191 resulting from the cleavage of the carbonyl-oxygen bond. Moreover, P12 (*trans*-5-*O*-*p*-coumaroylquinic acid) was distinguished by a base ion $[\text{QA-H}]^-$ at m/z 191 and an intense *p*-coumaric acid radical anion at m/z 163, which suggests that it probably involved both types of fragmentation pathways. These organic acids were identified by comparing the observed data (see Table 4) with reference data (Parveen et al., 2014).

3.4.4. Identification of the other compounds in EMF

Two anthraquinones were discovered in EMF. One was P44 (emodin), its precursor ion $[\text{M-H}]^-$ was observed at m/z 269, and it presented two main fragmentation ion peaks at m/z 241 and 225 (see Fig. 5 (E)), which corresponded to $[\text{M-H-CO}]^-$ and $[\text{M-H-CO}_2]^-$ ions. The other anthraquinone, P28 (anthraglycoside B, emodin-8-*O*-glucoside), demonstrated the loss of the glucose unit at m/z 431 \rightarrow 269 (see Table 4). P44 and P29 were identified as emodin and anthraglycoside B, respectively, after confirming with standards and references.

In recent years, scientists have looked towards nature for inspiration, and medicinal plants have become increasingly popular because of their pollution-free nature, low toxicity and side effects (Xiong 2011). Owing to their rich resources and multiple types of secondary metabolites,

Poaceae plants have broad prospects for development and utilization in the search for new drugs from natural sources. Many Poaceae plants have been used as medicinal plants for a long time. However, in addition to some well-known Chinese herbal medicines, such as *Coix lacryma-jobi* L., *Lophatherum gracile* Brongn., *Imperata cylindrica* (L.) Beauv. and other species, the majority of Poaceae medicinal plants have not attracted much attention; thus, related investigations are lacking (Xiong 2011). In the present study, 5 widely distributed species from the Poaceae family were collected, and their 95 % EtOH crude extracts were further prepared. The total flavonoid and total phenol contents of crude extracts were first tested because members of the Poaceae family are rich in flavonoids and phenols (Tohge et al., 2017, Xiang et al., 2019, Kiani et al., 2021). As a result, EMF was found to contain the highest total phenol and total flavonoid contents among all five tested samples.

AD and diabetes are two common chronic diseases that have attracted increased attention in the area of public health. Owing to the multifactorial pathogenesis of AD and diabetes, multitarget drugs are more effective therapeutic strategies for AD and diabetes treatment (Li et al., 2017). In recent decades, free radical and oxidative stress have become one of the most attractive subjects in scientific research (Stefanucci et al., 2020). Oxidative stress is an important pathological mechanism in AD and diabetes. The strategy of enzyme inhibition holds considerable promise in combating global health problems such as Alzheimer's disease (AD) and diabetes (Mollica et al., 2019). AChE and BChE are crucial targets that catalyze the breakdown of acetylcholine (ACh) and are implicated in the pathogenesis of AD. Thus, the development of AChE and BChE inhibitors is an effective way to intervene in the pathogenesis of AD (Tripathi et al., 2023). α -Amylase and α -glucosidase are two enzymes that are responsible for postprandial glucose levels (Baloglu et al., 2019). However, recent evidence has shown that significant inhibition of α -amylase is related to gastrointestinal disturbances caused by abnormal bacterial fermentation of undigested food in

the colon (Zhang et al., 2020). Therefore, treatment with a selective α -glucosidase inhibitor may generate a satisfactory therapeutic effect.

In the following experiments, we comprehensively evaluated the antioxidant and enzyme inhibitory activities of extracts from these five selected species. DPPH and ABTS assays are commonly used in *in vitro* models to evaluate the antioxidant activity of extracts (Mollica et al., 2019, Stefanucci et al., 2020). Therefore, we first chose these two assays to evaluate the antioxidant potential of the five samples. Surprisingly, EMF was found to have significant DPPH radical scavenging activity, with an IC_{50} value of $23.18 \pm 0.36 \mu\text{g/mL}$. In the enzyme inhibitory assays, the EMF showed obvious dural AChE (IC_{50} value = $49.92 \pm 1.44 \mu\text{g/mL}$) and BChE-inhibitory activities (IC_{50} value = $100.37 \pm 2.48 \mu\text{g/mL}$) and selective α -glucosidase-inhibitory activity (IC_{50} value = $50.01 \pm 2.15 \mu\text{g/mL}$). The above findings revealed the potential of EMF in the development of multi-targeted anti-AD and anti-diabetes drugs. Additionally, the results of the UV-visible spectrophotometer showed that the EMF contained high total phenol and total flavonoid contents. The above results indicated that the phenol/flavonoid contents and multiple tested activities may be positively correlated.

In the subsequent LC-IT-TOF-MS analysis, 44 compounds were identified from EMF, including 28 flavonoids and 13 organic acids; therefore, a majority of the identified compounds were phenols and flavonoids. UV-visible spectrophotometry and LC-IT-TOF-MS analysis confirmed their conclusions each other. According to literature, members of the genus *Miscanthus* are rich in flavonoids and phenolic acids (Mouri and Laursen 2011, Parveen et al., 2013, Parveen et al., 2014), and our results are consistent with previous phytochemical investigations. More importantly, we first identified anthraquinones from the genus *Miscanthus*, providing new data for further studies on this genus in plant chemotaxonomic research.

Flavonoids, such as isoorientin, isovitexin, cynaroside, luteolin, apigenin, diosmetin, rutin, quercetin, and eriodictyol, and phenolic acids, such as quinic acid and neochlorogenic acid, have been reported to exhibit free radical scavenging activity (Fraga et al., 1987, Zhan 1996, Bai et al., 2005, Cao et al., 2013). Isoorientin, isovitexin, quercetin, and 4-hydroxycinnamic acid possess dural AChE and BChE-inhibitory activities (Conforti et al., 2009, Khan et al., 2009, Szwajgier and Borowiec 2012). Additionally, related studies have demonstrated the glucosidase-inhibitory activities of luteolin, isoquercetin, quercetin, naringenin, and quinic acid (Iio et al., 1984, Matsui et al., 2004, Matsui et al., 2006, Shibano et al., 2008). On the basis of the related literature, flavonoids and phenolic acids present in the EMF may be responsible for its antioxidant, dural anti-AChE and anti-BChE activities and selected anti- α -glucosidase activities.

M. floridulus, widely distributed in tropical and subtropical regions, is rich in natural resources, and is easy to obtain (Xiong 2011). The plant is an industrial crop with multiple valuable applications, such as medicinal applications, soil fixation, papermaking, weaving, and greening (Xiong 2011). However, the medicinal value of this plant has not been thoroughly and systematically studied. The results obtained in the present study provide a new idea for the exploitation and utilization of *M. floridulus* in the pharmaceutical industry. *In vivo* experiments need to be performed to verify the multiple biological activities of *M. floridulus* in the future.

4. Conclusions

On the basis of bioactivity evaluations and phytochemical analyses of five Poaceae plants, *M. floridulus* was demonstrated to be a promising anti-AD and antidiabetic agent because of its significant antioxidant, dural AChE and BChE-inhibitory, and selective α -glucosidase-inhibitory activities. Therefore, *M. floridulus* is worthy of further study.

CRedit authorship contribution statement

Dingping Zhao: Writing – original draft, Validation, Methodology,

Investigation, Formal analysis. Qijun Dai: Methodology, Investigation, Formal analysis, Conceptualization. Yuanyuan Zhang: Methodology, Investigation, Formal analysis, Conceptualization. Hongjian Shen: Methodology, Investigation, Formal analysis, Conceptualization. Yan Mao: Methodology, Investigation, Formal analysis, Conceptualization. Xianxian Zhou: Methodology, Investigation, Formal analysis, Conceptualization. Xiqing Chen: Methodology, Investigation, Formal analysis, Conceptualization. Hanqing pang: Writing – review & editing, Methodology. Hui Wang: Project administration, Funding acquisition. Liang Liu: Writing – review & editing, Writing – original draft, Validation, Supervision, Project administration, Methodology, Funding acquisition.

Declaration of competing interest

The authors declare that they have no known competing financial interests or personal relationships that could have appeared to influence the work reported in this paper.

Acknowledgments

This research was funded by the High-end Talents Supporting Project of Yangzhou University and the Graduate Teaching Quality Engineering Project of Anhui Province (Grant No. 2023lhypsfd014). The authors thank Prof. Yuelin Song of Beijing University of Chinese Medicine for help with the LC-IT-TOF-MS analysis.

References

- Bai, N., Zhou, Z., Zhu, N., et al., 2005. Antioxidant flavonoids from the flower of *Inula britannica*. *J. Food Lipids* 12, 141–149. <https://doi.org/10.1111/j.1745-4522.2005.00012.x>.
- Balci, N., Çelik, H., Türkan, F., et al., 2023. Schiff base synthesis with a new reliable method and investigation of their inhibition effects on glutathione S-transferase and cholinesterase enzymes. *ChemistrySelect* 8, e202204566. <https://doi.org/10.1002/slct.202204566>.
- Baloglu, M.C., Llorent-Martinez, E.J., Aumeeruddy, M.Z., et al., 2019. Multidirectional insights on *Chrysophyllum perulchrum* leaves and stem bark extracts: HPLC-ESI-MSn profiles, antioxidant, enzyme inhibitory, antimicrobial and cytotoxic properties. *Ind. Crops Prod.* 134, 33–42. <https://doi.org/10.1016/j.indcrop.2019.03.066>.
- Boettcher, C., 2016. MassBank Europe. <https://massbank.eu/MassBank/RecordDisplay?id=MSBNK-IPB-Halle-PB000128&dsn=IPB-Halle> (accessed 13 March 2024).
- Cao, J., Xia, X., Dai, X., et al., 2013. Flavonoids profiles, antioxidant, acetylcholinesterase inhibition activities of extract from *Dryothyrum boryanum* (Willd.) Ching. *Food Chem. Toxicol.* 55, 121–128. <https://doi.org/10.1016/j.fct.2012.12.051>.
- Cetin, A., Bursal, E., Türkan, F., 2021. 2-methylindole analogs as cholinesterases and glutathione S-transferase inhibitors: Synthesis, biological evaluation, molecular docking, and pharmacokinetic studies. *Arab. J. Chem.* 14, 103449. <https://doi.org/10.1016/j.arabjc.2021.103449>.
- Conforti, F., Rigano, D., Menichini, F., et al., 2009. Protection against neurodegenerative diseases of *Iris pseudopumila* extracts and their constituents. *Fitoterapia* 80, 62–67. <https://doi.org/10.1016/j.fitote.2008.10.005>.
- Cuthbertson, D., Johnson, S., Lange, B., 2016. MassBank Europe. https://massbank.eu/MassBank/RecordDisplay?id=MSBNK-Washington_State_University-BML00330&dsn=Washington_State_University (accessed 4 May 2024).
- El Molla, S.G., Abdel Motal, A., El Hefnawy, H., et al., 2016. Cytotoxic activity of phenolic constituents from *Echinochloa crus-galli* against four human cancer cell lines. *Rev. Bras. Farmacogn.* 26, 62–67. <https://doi.org/10.1016/j.bjp.2015.07.026>.
- Ferreira-Vieira, T.H., Guimaraes, I.M., Silva, F.R., et al., 2016. Alzheimer's disease: Targeting the cholinergic system. *Curr. Neuropharmacol.* 14 (1), 101–115. <https://doi.org/10.2174/1570159x13666150716165726>.
- Fraga, C.G., Martino, V.S., Ferraro, G.E., et al., 1987. Flavonoids as antioxidants evaluated by *in vitro* and *in situ* liver chemiluminescence. *Biochem. Pharmacol.* 36, 717–720. [https://doi.org/10.1016/0006-2952\(87\)90724-6](https://doi.org/10.1016/0006-2952(87)90724-6).
- Fujian Institute of Medicine, 1970. *Fujian Chinese Herbal Medicine*. Fujian Institute of Medicine, Fujian.
- Gallaher, T.J., Peterson, P.M., Soreng, R.J., et al., 2022. Grasses through space and time: An overview of the biogeographical and macroevolutionary history of Poaceae. *J. Syst. Evol.* 60, 522–569. <https://doi.org/10.1111/jse.12857>.
- Grochowski, D.M., Uysal, S., Aktumsek, A., et al., 2017. *In vitro* enzyme inhibitory properties, antioxidant activities, and phytochemical profile of *Potentilla thuringiaca*. *Phytochem. Lett.* 20, 365–372. <https://doi.org/10.1016/j.phytol.2017.03.005>.
- Huang, W., Zhang, L., Columbus, J.T., et al., 2022. A well-supported nuclear phylogeny of Poaceae and implications for the evolution of C(4) photosynthesis. *Mol. Plant.* 15, 755–777. <https://doi.org/10.1016/j.molp.2022.01.015>.
- Iio, M., Yoshioka, A., Imayoshi, Y., et al., 1984. Effect of flavonoids on α -glucosidase and β -fructosidase from yeast. *Agric. Biol. Chem.* 48, 1559. <https://doi.org/10.1080/00021369.1984.10866342>.

- Ji, H.Y., Lee, H.W., Shim, H.J., et al., 2004. Metabolism of eupatilin in rats using liquid chromatography/electrospray mass spectrometry. *Biomed. Chromatogr.* 18, 173–177. <https://doi.org/10.1002/bmc.307>.
- Kakazu, Y., Horai, H., 2016. MassBank Europe. https://massbank.eu/MassBank/RecordDisplay?id=MSBNK-Keio_Univ-KO000864&dsn=Keio_Univ (accessed 7 April 2024).
- Kang, K. B., 2018. MassBank of North America. <https://mona.fiehnlab.ucdavis.edu/spectra/display/CCMSLIB00004679279> (accessed 7 March 2024).
- Khan, M.T., Orhan, I., Senol, F.S., et al., 2009. Cholinesterase inhibitory activities of some flavonoid derivatives and chosen xanthone and their molecular docking studies. *Chem. Biol. Interact.* 181, 383–389. <https://doi.org/10.1016/j.cbi.2009.06.024>.
- Kiani, R., Arzani, A., Mirmohammady Maibody, S.A.M., 2021. Polyphenols, flavonoids, and antioxidant activity involved in salt tolerance in wheat, *Aegilops cylindrica* and their amphidiploids. *Front Plant Sci.* 12, 646221. <https://doi.org/10.3389/fpls.2021.646221>.
- Kohlhoff, M., 2016. MassBank Europe. <https://massbank.eu/MassBank/RecordDisplay?id=MSBNK-Fiocruz-FIO00087&dsn=Fiocruz> (accessed 14 March 2024).
- Kohlhoff, M., 2016. MassBank Europe. <https://massbank.eu/MassBank/RecordDisplay?id=MSBNK-Fiocruz-FIO00064&dsn=Fiocruz> (accessed 11 May 2024).
- Kohlhoff, M., 2016. MassBank Europe. <https://massbank.eu/MassBank/RecordDisplay?id=MSBNK-Fiocruz-FIO000741&dsn=Fiocruz> (accessed 14 April 2024).
- Lahiri, D.K., Farlow, M.R., Sambamurti, K., et al., 2003. A critical analysis of new molecular targets and strategies for drug developments in Alzheimer's disease. *Curr. Drug Targets* 4 (2), 97–112. <https://doi.org/10.2174/1389450033346957>.
- Li, Q., Tu, Y., Zhu, C., et al., 2017. Cholinesterase, β -amyloid aggregation inhibitory and antioxidant capacities of Chinese medicinal plants. *Ind. Crops Prod.* 108, 512–519. <https://doi.org/10.1016/j.indcrop.2017.07.001>.
- Liu, L., Gao, Q., Zhang, Z., et al., 2022. *Elsholtzia rugulosa*: Phytochemical profile and antioxidant, anti-Alzheimer's disease, antidiabetic, antibacterial, cytotoxic and hepatoprotective activities. *Plant Foods Hum. Nutr.* 77, 62–67. <https://doi.org/10.1007/s11130-021-00941-4>.
- Mala, P., Khan, G.A., Gopalan, R., et al., 2022. Fijian medicinal plants and their role in the prevention of Type 2 diabetes mellitus. *Biosci. Rep.* 42, 11. <https://doi.org/10.1042/bsr20220461>.
- Matsuda, F., Suzuki, M. and Sawada, Y., 2009. MassBank of North America. <https://mona.fiehnlab.ucdavis.edu/spectra/display/PT208460> (accessed 25 March 2024).
- Matsuda, F., Suzuki, M. and Sawada, Y., 2009. MassBank of North America. <https://mona.fiehnlab.ucdavis.edu/spectra/display/PT202000> (accessed 19 April 2024).
- Matsuda, F., Suzuki, M. and Sawada, Y., 2016. MassBank Europe. <https://massbank.eu/MassBank/RecordDisplay?id=MSBNK-RIKEN-PR100727&dsn=RIKEN> (accessed 24 April 2024).
- Matsuda, F., 2016. MassBank Europe. <https://massbank.eu/MassBank/RecordDisplay?id=MSBNK-RIKEN-PRO40016&dsn=RIKEN> (accessed 18 April 2024).
- Matsuda, F., 2016. MassBank Europe. <https://massbank.eu/MassBank/RecordDisplay?id=MSBNK-RIKEN-PRO40059&dsn=RIKEN> (accessed 21 March 2024).
- Matsuda, F., 2016. MassBank Europe. <https://massbank.eu/MassBank/RecordDisplay?id=MSBNK-MSSJ-MSJ00022&dsn=MSSJ> (accessed 23 April 2024).
- Matsuda, F., 2016. MassBank Europe. <https://massbank.eu/MassBank/RecordDisplay?id=MSBNK-RIKEN-PRO40032&dsn=RIKEN> (accessed 13 May 2024).
- Matsui, T., Ebuichi, S., Fujise, T., et al., 2004. Strong antihyperglycemic effects of water-soluble fraction of Brazilian propolis and its bioactive constituent, 3,4,5-tri-O-cafeoylquinic acid. *Biol. Pharm. Bull.* 27, 1797–1803. <https://doi.org/10.1248/bpb.27.1797>.
- Matsui, T., Ogunwande, I.A., Abesundara, K.J., et al., 2006. Anti-hyperglycemic potential of natural products. *Mini Rev. Med. Chem.* 6, 349–356. <https://doi.org/10.2174/138955706776073484>.
- Meng, Y., Su, A., Yuan, S., et al., 2016. Evaluation of total flavonoids, myricetin, and quercetin from *Hovenia dulcis* Thunb. as inhibitors of α -amylase and α -glucosidase. *Plant Foods Hum. Nutr.* 71, 444–449. <https://doi.org/10.1007/s11130-016-0581-2>.
- Mollica, A., Stefanucci, A., Macedonio, G., et al., 2019. Chemical composition and biological activity of *Capparis spinosa* L. from Lipari Island. *S. Afr. J. Bot.* 120, 135–140. <https://doi.org/10.1016/j.sajb.2018.02.397>.
- Mouri, C., Laursen, R., 2011. Identification and partial characterization of C-glycosylflavone markers in Asian plant dyes using liquid chromatography-tandem mass spectrometry. *J. Chromatogr. A* 1218, 7325–7330. <https://doi.org/10.1016/j.chroma.2011.08.048>.
- Nessa, F., Ismail, Z., Mohamed, N., et al., 2004. Free radical-scavenging activity of organic extracts and of pure flavonoids of *Blumea balsamifera* DC leaves. *Food Chem.* 88, 243–252. <https://doi.org/10.1016/j.foodchem.2004.01.041>.
- Ong, S.L., Nalamolu, K.R., Lai, H.Y., 2017. Potential lipid-lowering effects of *Eleusine indica* (L) Gaertn. extract on high-fat-diet-induced hyperlipidemic rats. *Pharmacogn. Mag.* 13, S1–S9. <https://doi.org/10.4103/0973-1296.203986>.
- Parveen, I., Threadgill, M.D., Hauck, B., et al., 2011. Isolation, identification and quantitation of hydroxycinnamic acid conjugates, potential platform chemicals, in the leaves and stems of *Miscanthus × giganteus* using LC-ESI-MSn. *Phytochemistry* 72, 2376–2384. <https://doi.org/10.1016/j.phytochem.2011.08.015>.
- Parveen, I., Wilson, T., Donnison, I.S., et al., 2013. Potential sources of high value chemicals from leaves, stems and flowers of *Miscanthus sinensis* 'Goliath' and *Miscanthus sacchariflorus*. *Phytochemistry* 92, 160–167. <https://doi.org/10.1016/j.phytochem.2013.04.004>.
- Parveen, I., Wilson, T., Threadgill, M.D., et al., 2014. Screening for potential co-products in a *Miscanthus sinensis* mapping family by liquid chromatography with mass spectrometry detection. *Phytochemistry* 105, 186–196. <https://doi.org/10.1016/j.phytochem.2014.05.003>.
- Phelan, V., 2019. The Human Metabolome Database. https://hmdb.ca/spectra/ms_ms/374655 (accessed 16 May 2024).
- Qneibi, M., Hanania, M., Jaradat, N., et al., 2021. *Inula viscosa* (L.) Greuter, phytochemical composition, antioxidant, total phenolic content, total flavonoids content and neuroprotective effects. *Eur. J. Integr. Med.* 42, 101291. <https://doi.org/10.1016/j.eujim.2021.101291>.
- Sánchez-Rabeneda, F., Jáuregui, O., Casals, I., et al., 2003. Liquid chromatographic/electrospray ionization tandem mass spectrometric study of the phenolic composition of cocoa (*Theobroma cacao*). *J. Mass Spectrom.* 38, 35–42. <https://doi.org/10.1002/jms.395>.
- Sawada, Y., Matsuda, F., Hirai, M., 2008. MassBank of North America. <https://mona.fiehnlab.ucdavis.edu/spectra/display/PS101107> (accessed 19 May 2024).
- Schulze, T., 2017. MassBank Europe. https://massbank.eu/MassBank/RecordDisplay?id=MSBNK-BGC_Munich-RP016812&dsn=BGC_Munich (accessed 2 May 2024).
- Shibano, M., Kakutani, K., Taniguchi, M., et al., 2008. Antioxidant constituents in the dayflower (*Commelina communis* L.) and their α -glucosidase-inhibitory activity. *J. Nat. Med.* 62, 349–353. <https://doi.org/10.1007/s11418-008-0244-1>.
- Silva, D., 2014. MassBank of North America. <https://mona.fiehnlab.ucdavis.edu/spectra/display/CCMSLIB00000077236> (accessed 7 May 2024).
- Silva, D., 2019. The Human Metabolome Database. https://hmdb.ca/spectra/ms_ms/374065 (accessed 16 May 2024).
- Stefanucci, A., Zengin, G., Llorent-Martinez, E.J., et al., 2020. *Viscum album* L. homogenizer-assisted and ultrasound-assisted extracts as potential sources of bioactive compounds. *J. Food Biochem.* 44, e13377. <https://doi.org/10.1111/jfbc.13377>.
- Szwaigier, D., Borowiec, K., 2012. Phenolic acids from malt are efficient acetylcholinesterase and butyrylcholinesterase inhibitors. *J. Int. Brew.* 118, 40–48. <https://doi.org/10.1002/jib.5>.
- Tetsuya, M., 2019. MassBank of North America. <https://mona.fiehnlab.ucdavis.edu/spectra/display/PR309126> (accessed 23 May 2024).
- Tohge, T., de Souza, L.P., Fernie, A.R., 2017. Current understanding of the pathways of flavonoid biosynthesis in model and crop plants. *J. Exp. Bot.* 68, 4013–4028. <https://doi.org/10.1093/jxb/erx177>.
- Tripathi, M.K., Bhardwaj, B., Waiker, D.K., et al., 2023. Discovery of novel dual acetylcholinesterase and butyrylcholinesterase inhibitors using machine learning and structure-based drug design. *J. Mol. Struct.* 1286, 135517. <https://doi.org/10.1016/j.molstruc.2023.135517>.
- Wang, M., 2017. MassBank of North America. <https://mona.fiehnlab.ucdavis.edu/spectra/display/CCMSLIB00000848118> (accessed 27 May 2024).
- Waridel, P., Wolfender, J.L., Ndjoko, K., et al., 2001. Evaluation of quadrupole time-of-flight tandem mass spectrometry and ion-trap multiple-stage mass spectrometry for the differentiation of C-glycosidic flavonoid isomers. *J. Chromatogr. A* 926, 29–41. [https://doi.org/10.1016/s0021-9673\(01\)00806-8](https://doi.org/10.1016/s0021-9673(01)00806-8).
- Wishart, D., Tzur, D., Knox, C., 2007. The Human Metabolome Database. https://hmdb.ca/spectra/ms_ms/1479355 (accessed 26 March 2024).
- Xiang, J., Apea-Bah, F.B., Ndolo, V.U., et al., 2019. Profile of phenolic compounds and antioxidant activity of finger millet varieties. *Food Chem.* 275, 361–368. <https://doi.org/10.1016/j.foodchem.2018.09.120>.
- Xiong, L., 2011. Studies on the Chemical Constituents and Biological Activities of *Miscanthus floridulus*, Master. The Second Military Medical University.
- Xu, R., Bu, Y.G., Zhao, M.L., et al., 2020. Studies on antioxidant and α -glucosidase inhibitory constituents of Chinese toon bud (*Toona sinensis*). *J. Funct. Foods* 73, 104108. <https://doi.org/10.1016/j.jff.2020.104108>.
- Yilmaz, M.A., Taslimi, P., Kılıç, Ö., et al., 2023. Unravelling the phenolic compound reserves, antioxidant and enzyme inhibitory activities of an endemic plant species, *Achillea pseudoaleppica*. *J. Biomol. Struct. Dyn.* 41 (2), 445–456. <https://doi.org/10.1080/07391102.2021.2007792>.
- Zhan, P., 1996. Study on antioxidant activity of extracts from sweet potato and potato. *Food Ferment. Ind.* 2, 30–33. https://kns.cnki.net/kcms2/article/abstract?v=O9dCEmDP74JfGmAbcdnLwteQCF59j4baK2K5H-WHZJ_Vob55q5tnF4PP0rE9CFHyx7knaWb5T3zqJb0eyXlXzF9r27XYQ9Y5mx98SfpV3_FVxvXiEbx3nkX_x_ydAxQmjCABY=&uniplatform=NZKPT&language=CHS.
- Zhang, Z., Dai, L., Wang, H., et al., 2021. Phytochemical profiles and antioxidant, anticholinergic, and antidiabetic activities of *Odontites serotina* (Lam.) Dum. *Eur. J. Integr. Med.* 44, 101340. <https://doi.org/10.1016/j.eujim.2021.101340>.
- Zhang, J., Ma, C., Zhu, S., 2008. Effects of dietary fiber in oat bran on blood glucose and blood lipid in experimental type-2 diabetes mellitus rats. *J. Shanxi Datong Univ. (Nat. Sci.)* 24, 64–67. https://kns.cnki.net/kcms2/article/abstract?v=O9dCEmDP74JfGmAbcdnLwteQCF59j4baK2K5H-WHZJ_Vob55q5tnF4PP0rE9CFHyx7knaWb5T3zqJb0eyXlXzF9r27XYQ9Y5mx98SfpV3_FVxvXiEbx3nkX_x_ydAxQmjCABY=&uniplatform=NZKPT&language=CHS.
- Zhang, L., Rocchetti, G., Zengin, G., et al., 2020. Profiling of polyphenols and sesquiterpenoids using different extraction methods in *Muscari turcicum*, an endemic plant from Turkey. *Ind. Crops Prod.* 154, 112626. <https://doi.org/10.1016/j.indcrop.2020.112626>.
- Zhao, D., Chen, X., Wang, R., et al., 2023. Determining the chemical profile of *Caragana jubata* (Pall.) Poir. by UPLC-QTOF-MS analysis and evaluating its anti-ischemic stroke effects. *J. Ethnopharmacol.* 309, 116275. <https://doi.org/10.1016/j.jep.2023.116275>.
- Zou, M., Wang, R., Yin, Q., et al., 2021. Bioassay-guided isolation and identification of anti-Alzheimer's active compounds from *Spiranthes sinensis* (Pers.) Ames. *Med. Chem. Res.* 30, 1849–1855. <https://doi.org/10.1007/s00044-021-02777-8>.